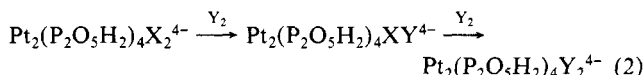
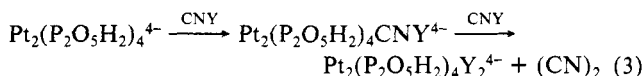


namically unfavorable. Scheme I shows the thermal replacement reactions that occur with halogens and halides. If small quantities of Y_2 are added to $Pt_2(P_2O_5H_2)_4X_2^{4-}$ the initial formation of $Pt_2(P_2O_5H_2)_4XY^{4-}$ can be verified (eq 2). With interhalogens

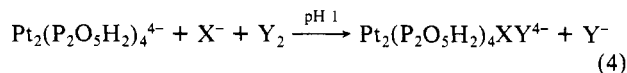


(XY) and $Pt_2(P_2O_5H_2)_4^{4-}$ the first product is $Pt_2(P_2O_5H_2)_4XY^{4-}$ (XY = CH_3I ,¹⁰ ICl, IBr, CNBr, CNI), but if excess XY is added the major product is $Pt_2(P_2O_5H_2)_4Y_2^{4-}$ (eq 3).¹⁹ No evidence



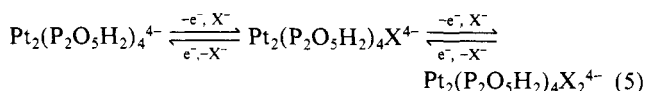
is found for $Pt_2(P_2O_5H_2)_4X_2$ (X = CH_3 , CN, I (from ICl, IBr)), which correlates with $E^\circ(Cl_2/Cl^-) > E^\circ(Br_2/Br^-) > E^\circ(I_2/I^-) > E^\circ((CN)_2/CN^-)$.

Using techniques of Pt(IV) chemistry,²⁰ we can use a novel method to prepare stable aqueous solutions of the mixed complexes $Pt_2(P_2O_5H_2)_4XY^{4-}$ (X = Cl, Y = Br, I; X = Br, Y = I) in high yield. This complementary redox process²¹ involves treating an aqueous mixture of halide (X^-) and $Pt_2(P_2O_5H_2)_4^{4-}$ at low pH with a small quantity of halogen Y_2 (X = Cl, Y = Br, I; X = Br, Y = I) (eq 4).



At this low pH the solutions are stable since $[Y^-]$ is low and the substitution rate is slow. Respective λ_{max} are ClBr 298 nm (ϵ 5.6×10^4), ClI 313 nm (ϵ 4.1×10^4), BrI 316 nm (ϵ 5.2×10^4). The ³¹P NMR spectra correspond with the XY compounds formed by eq 2.

Although reversible electrochemistry has not been observed because of electrode adsorption, chemical reduction of $Pt_2(P_2O_5H_2)_4^{4-}$ to $Pt_2(P_2O_5H_2)_4^{6-}$ occurs with Cr(II).²² Electrochemical oxidation of a solution of $Pt_2(P_2O_5H_2)_4^{4-}$ and X^- (X = Cl, Br, I) at pH 1-2 with a Pt gauze electrode at + 0.8 V vs. Ag/AgCl gives $Pt_2(P_2O_5H_2)_4X_2^{4-}$. At 0.0 V, or with added H_2 , H_3PO_2 , or Zn/Hg, the reaction is reversed. For conditions where $[Pt_2(P_2O_5H_2)_4^{4-}] = [Pt_2(P_2O_5H_2)_4X_2^{4-}]$, we find E° (X = Cl) = 0.20, E° (X = Br) = 0.066, and E° (X = I) = -0.146 V vs. SCE. This low potential for oxidation of $Pt_2(P_2O_5H_2)_4^{4-}$ correlates with electron loss from a $d\sigma^*$ HOMO. The one-electron oxidants Ce^{4+} and $IrCl_6^{2-}$ can also be used to effect this oxidation (eq 5), and



a Ce^{4+} titration verifies that $n = 2$ for the oxidation.²³ If we assume an initial 1-electron process, removal of a $1a_{2u}$ ($d\sigma^*$) electron from $Pt_2(P_2O_5H_2)_4^{4-}$ gives $Pt_2(P_2O_5H_2)_4^{3-}$, which with excess X^- will form the mixed-valence complex $Pt_2(P_2O_5H_2)_4X^{4-}$.

(19) For $Pt_2(P_2O_5H_2)_4CNBr^{4-}$: $\lambda_{max} = 279, 344$ nm; $\nu(CN) = 2152.6$ cm^{-1} ; ³¹P NMR δ 26.08 (¹J(¹⁹⁵Pt³¹P) = 2230 Hz), 16.58 (¹J(¹⁹⁵Pt³¹P) = 1993 Hz); ¹⁹⁵Pt NMR -4593 (¹J(¹⁹⁵Pt³¹P) = 2224, ²J(¹⁹⁵Pt³¹P) = 102 Hz), -4101 (¹J(¹⁹⁵Pt³¹P) = 1988, ²J(¹⁹⁵Pt³¹P) = 67 Hz). For $Pt_2(P_2O_5H_2)_4CNI^{4-}$: $\lambda_{max} = 294, 356$ nm; $\nu(CN) = 2151.7$ cm^{-1} ; ³¹P NMR δ 19.96 (¹J(¹⁹⁵Pt³¹P) = 2219 Hz), 15.40 (¹J(¹⁹⁵Pt³¹P) = 2006 Hz); ¹⁹⁵Pt NMR δ -5087 (¹J(¹⁹⁵Pt³¹P) = 2218, ²J(¹⁹⁵Pt³¹P) = 92 Hz), -4028 (¹J(¹⁹⁵Pt³¹P) = 1934, ²J(¹⁹⁵Pt³¹P) = 57 Hz). For $Pt_2(P_2O_5H_2)_4BrCl^{4-}$: ³¹P NMR δ 27.42 (¹J(¹⁹⁵Pt³¹P) = 2151 Hz), 24.38 (¹J(¹⁹⁵Pt³¹P) = 2153 Hz). For $Pt_2(P_2O_5H_2)_4ICl^{4-}$: ³¹P NMR δ 26.47 (¹J(¹⁹⁵Pt³¹P) = 2236 Hz), 19.46 (¹J(¹⁹⁵Pt³¹P) = 2175 Hz).

(20) Peloso, A. *Coord. Chem. Rev.* **1973**, *10*, 123-181.
(21) Chanon, M.; Tobe, M. L. *Angew. Chem., Int. Ed. Engl.* **1982**, *21*, 1-23.

(22) Alexander, K. A.; Stein, P.; Hedden, D. B.; Roundhill, D. M. *Polyhedron* **1983**, *2*, 1389-1392.

(23) Since the Ce^{4+} oxidation of Cl^- is kinetically slow (see: Skoog, D. A.; West, D. M. "Fundamentals of Analytical Chemistry", 3rd ed.; Holt, Rinehart and Winson: New York, 1976; p 347), we can discount the pathway where Cl^- is oxidized rather than $Pt_2(P_2O_5H_2)_4^{4-}$.

Since solutions of $Pt_2(P_2O_5H_2)_4X^{4-}$ rapidly disproportionate¹¹ the product $Pt_2(P_2O_5H_2)_4X_2$ can result either from this reaction or from transfer of a second electron to the oxidant followed by halide ion capture.

We are currently doing kinetic measurements and quantum yield experiments to mechanistically probe these reactions.

Acknowledgment. We thank Pinky Tivari for experimental assistance. We thank the Boeing Co for financial support to purchase the Nicolet 200-MHz NMR spectrometer (WSU).

Virtual Transition State for the Acylation Step of Acetylcholinesterase-Catalyzed Hydrolysis of *o*-Nitrochloroacetanilide¹

Daniel M. Quinn* and Michael L. Swanson

Department of Chemistry, University of Iowa
Iowa City, Iowa 52242

Received November 18, 1983

Acetylcholinesterase (AChE) catalysis² occurs via an acyl-enzyme mechanism involving nucleophilic attack by serine on the substrate, with general acid-base assistance by histidine. Rosenberry^{2,3} suggested that small solvent deuterium isotope effects (<1.5) and low pK_a 's (<6) for k_{cat}/K_m of the AChE-catalyzed hydrolyses of neutral acetate esters arise because a pH-insensitive, nonchemical step (induced fit) preceding general acid-base catalysis figures prominently in rate determination. The low pK_a 's were considered to result from reduction of the intrinsic $pK_a = 6.3$ of the catalytic histidine by a kinetic term containing the rate constant of the pH-insensitive step (vide infra). When more than a single elementary step contributes to rate determination, the observed transition state is a virtual transition state,^{4,5} for which phenomenological descriptors of structure, such as solvent isotope effects, contain weighted contributions from the requisite elementary step transition states. In this communication we show that the acylation transition state of the AChE-catalyzed hydrolysis of *o*-nitrochloroacetanilide⁶ (ONCA) is a virtual transition state and dissect the virtual transition state into its component transition states.

Figure 1 shows that, as for Rosenberry's ester substrates,³ pL -rate profiles (L = H, D) for the acylation step of AChE-catalyzed hydrolysis of ONCA yield small solvent isotope effects and low pK_a 's. The least-squares calculated pK_a 's are 5.77 ± 0.02 and 6.17 ± 0.02 in H_2O and D_2O , respectively, and the isotope effect on the least-squares extrapolated limiting velocity is 1.357 ± 0.007 . Figure 2 shows that the partial solvent isotope effect determined in mixed H_2O - D_2O buffers varies in a bowing upward manner with increasing mole fraction of deuterium, similar to the dependence reported by Hogg et al.⁷ for acylation of AChE by *p*-nitrophenyl acetate. The general expression for the dependence of rate constant on mole fraction of deuterium in the solvent is given by the Gross-Butler equation:⁸⁻¹⁰

$$k_n = k^{H_2O} \frac{\prod_j (1 - n + n\Phi_j^T)}{\prod_i (1 - n + n\Phi_i^R)} \quad (1)$$

(1) This work was supported by a Junior Faculty Biomedical Research Support Grant to D.M.Q. from the University of Iowa Research Council.

(2) Rosenberry, T. L. *Adv. Enzymol. Relat. Areas Mol. Biol.* **1975**, *43*, 103-218.

(3) Rosenberry, T. L. *Proc. Natl. Acad. Sci. U.S.A.* **1975**, *72*, 3834-3838.

(4) Schowen, R. L. In "Transition States of Biochemical Processes"; Gandour, R. D., Schowen, R. L., Eds.; Plenum Press: New York, 1978; pp 77-114.

(5) Stein, R. L. *J. Org. Chem.* **1981**, *46*, 3328-3330.

(6) Naveh, M.; Bernstein, Z.; Segal, D.; Shalitin, Y. *FEBS Lett.* **1981**, *134*, 53-56.

(7) Hogg, J. L.; Elrod, J. P.; Schowen, R. L. *J. Am. Chem. Soc.* **1980**, *102*, 2082-2086.

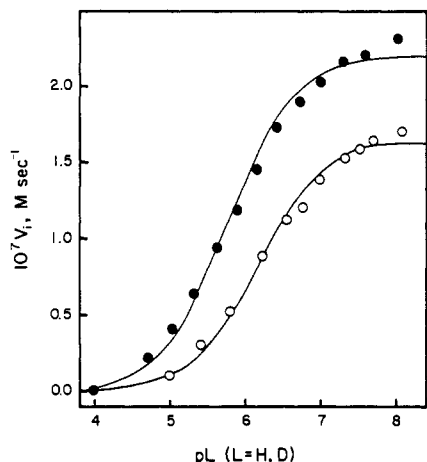
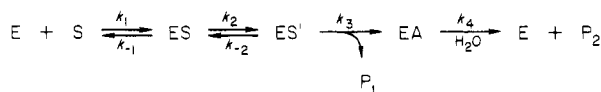


Figure 1. Dependence of initial velocity of AChE-catalyzed hydrolysis of ONCA on pL (L = H, D) at 25.0 ± 0.1 °C. Each run contained 0.1 M NaCl, 0.1 mM substrate ($= 0.12K_m$), 0.1 M buffer, and $7.1 \mu\text{g}$ of electric eel AChE (Sigma Chemical Co.) in 1.00-mL total volume. Buffers were acetic acid/sodium acetate ($\text{pH} < 5.5$, $\text{pD} < 6$) and $\text{NaH}_2\text{PO}_4/\text{Na}_2\text{HPO}_4$ ($\text{pH} > 5.7$, $\text{pD} > 6$). Time courses of substrate hydrolysis were obtained by monitoring *o*-nitroaniline production at 413 nm with a Beckman DU7 UV-vis spectrophotometer. Each point is the mean of at least two determinations, with an average precision of the means of $\pm 1.94\%$ in D_2O and $\pm 1.77\%$ in H_2O . Curvilinear lines are least-squares fits to the function $V_i = V_{i,\text{lim}}K_a/([\text{H}^+] + K_a)$. (●) Initial velocities in H_2O , (○) initial velocities in D_2O .

Scheme I



$$k_E = V_{\text{max}}/K_m = \frac{k_1 k_2 k_3}{k_{-1}(k_{-2} + k_3)} [\text{E}]_T : \text{EA} = \text{acylenzyme}$$

When more than a single step of the acylation mechanism contributes to rate determination, the minimal AChE mechanism is that of Scheme I. The nonlinear plot of Figure 2 can be interpreted in terms of changes in contributions to rate determination of serial transition states in D_2O vs. H_2O . For example, consider a model in which only the k_3 step of the AChE acylation mechanism is isotopically sensitive. The Gross-Butler equation for the k_3 step, assuming⁸ all Φ_i^{R} 's = 1 and a single transition-state proton contributes to the solvent isotope effect, is

$$k_{3,n} = k_3^{\text{H}_2\text{O}}(1 - n + n\Phi^{\text{T}}) \quad (2)$$

Substitution of this equation into V_{max}/K_m of Scheme I gives eq 3. In eq 3, $C = k_3^{\text{H}_2\text{O}}/k_{-2}$ and, borrowing Northrop's¹¹ terminology,

$$k_{E,n}/k_{E}^{\text{D}_2\text{O}} = \frac{(1 - n + n\Phi^{\text{T}})(1 + C\Phi^{\text{T}})}{\Phi^{\text{T}} + C\Phi^{\text{T}}(1 - n + n\Phi^{\text{T}})} \quad (3)$$

is called the commitment to proton-transfer catalysis. C measures the tendency for ES' to revert to ES or to continue to the acylenzyme.

A least-squares fit of the data of Figure 2 to eq 3 gives $C = 2.46 \pm 0.09$ and $\Phi^{\text{T}} = 0.41 \pm 0.01$. The commitment to proton-transfer catalysis indicates that the k_3 step is 2.46 times faster than the k_{-2} step. Hence, the k_2 transition state (which is the k_{-2} transition state) makes a 71% contribution (i.e., $100 \times 2.46/(2.46 + 1)$) and the k_3 transition state a 29% contribution to the virtual

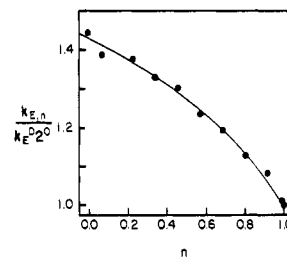
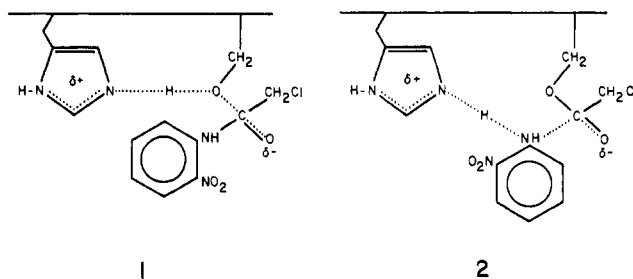


Figure 2. Dependence of partial solvent isotope effect at pH 7.30 and equivalent⁸ on atom fraction of solvent deuterium in 0.1 M sodium phosphate buffer at 25.0 ± 0.1 °C. Each run contained 0.1 M NaCl and $14 \mu\text{g}$ of electric eel AChE (Sigma Chemical Co.) in 1.00-mL total volume. First-order rate constants for ONCA hydrolysis were calculated by nonlinear least-squares fitting of 600 $\{A, t\}$ pairs to the function $A = \Delta A e^{-kt} + A_\infty$, where A is the absorbance at 413 nm, t is time, k is the first-order rate constant ($= V_{\text{max}}/K_m$), $\Delta A = A_0 - A_\infty$, and A_0 and A_∞ are the absorbances at $t = 0$ and $t = \infty$, respectively. Initial substrate concentration was 0.04 mM ($= K_m/21$) and reactions were followed for > 4 half-lives. At least two determinations were done at each atom fraction. The average precision of the rate constants is $\pm 0.48\%$. The plotted curve is a least-squares fit to eq 3 of the text.

transition state of the acylation step. The solvent isotope effect for the k_3 step is $1/0.41 = 2.44$, which is similar to that for deacylation of acetyl-AChE³ (which depends on a $\text{p}K_a = 6.3$, the intrinsic $\text{p}K_a$ of the active-site histidine). The transition state of the k_3 step thus appears to be stabilized by a general acid-base proton bridge, as in structures 1 and 2. The commitment to



proton-transfer catalysis calculated herein also allows calculation of the intrinsic $\text{p}K_a$ of the titrating active site residue from the observed $\text{p}K_a$ of the pH-rate profile of Figure 1. Similar to Rosenberry's^{2,3} account of the effect of incursion to rate determination by a pH-insensitive induced-fit step, one can show that the commitment to proton-transfer catalysis gives the following relationship for observed and intrinsic $\text{p}K_a$'s:¹²

$$\text{p}K_a^{\text{int}} = \text{p}K_a^{\text{obsd}} + \log(1 + k_3^{\text{H}_2\text{O}}/k_{-2}) \quad (4)$$

The intrinsic $\text{p}K_a$ calculated from eq 4 is 6.31, in excellent agreement with the long-postulated $\text{p}K_a$ of the active-site histidine.

In summary, acylation of AChE by ONCA is rate limited by a virtual transition state comprised of a solvent-isotope-insensitive and pH-insensitive transition state and a pH-sensitive transition state that is stabilized by general acid-base proton bridging.¹³ An important question remains: Is the k_2 step transition state that for a chemical or a physical process? Investigation continues in our laboratory on this question.

(12) Equation 4 is the decimal logarithm transform of an equation derived by Rosenberry^{2,3} that describes the effect on the observed $\text{p}K_a$ of partial rate determination by a pH-insensitive step preceding general acid-base catalysis in the AChE acylation mechanism.

(13) Like phenyl acetate² ($k_{\text{cat}}/K_m = 7.9 \times 10^6 \text{ M}^{-1} \text{ s}^{-1}$), the less reactive ONCA⁶ ($k_{\text{cat}}/K_m = 1.1 \times 10^4 \text{ M}^{-1} \text{ s}^{-1}$) acylates AChE primarily via a pH-insensitive and solvent-isotope-insensitive rate-limiting step. One might have expected the general acid-base transition state(s) of AChE acylation catalysis to be rate determining for the less reactive anilide substrate. However, acylation of AChE by neutral carbamoylating agents (which resembles the acylation step of catalysis) is also rate limited by a pH-insensitive step, though the carbamoylation rate constants are in the range (4.8×10^1)–(9×10^3) $\text{M}^{-1} \text{ s}^{-1}$: Reiner, E.; Aldridge, W. N. *Biochem. J.* 1967, 105, 171–179.

(8) Schowen, K. B. J. In "Transition States of Biochemical Processes"; Gandour, R. D., Schowen, R. L., Eds.; Plenum Press: New York, 1978; pp 225–283.

(9) Gold, V. *Adv. Phys. Org. Chem.* 1969, 7, 259–331.

(10) Schowen, R. L. *Prog. Phys. Org. Chem.* 1972, 9, 275–332.

(11) Northrop, D. B. In "Isotope Effects on Enzyme-Catalyzed Reactions"; Cleland, W. W., O'Leary, M. H., Northrop, D. B., Eds.; University Park Press: Baltimore, 1977; pp 122–152.